Wire Composition: Its Effect on Metal Disintegration and Particle Formation in Twin-Wire Arc-Spraying Process

W. Tillmann and M. Abdulgader

The wire tips in twin-wire arc-spraying (TWAS) are heated in three different zones. A high-speed camera was used to observe the melting behavior, metal breakup, and particle formation under different operating conditions. In zone (I), the wire tips are melted (liquidus metal) and directly atomized in the form of smaller droplets. Their size is a function of the specific properties of the molten metal and the exerting aerodynamic forces. Zone (II) is directly beneath zone (I) and the origin of the extruded metal sheets at the wire tips. The extruded metal sheets in the case of cored wires are shorter than those observed while using solid wires. In this study, the effects of adjustable parameters and powder filling on melting behavior, particle formation, and process instability were revealed, and a comparison between solid and cored wires was made. The findings can improve the accuracy of the TWAS process modeling.

1. Introduction

A heat source is utilized in thermal-spraying processes to melt the feedstock. The molten or semi-molten material is propelled toward a prepared substrate surface by expansion of the process and atomization gases. The subsequent impact of the in-flight particles on the substrate generates a coating. Therefore, the efficiency of a thermal-spraying process is dependent on the energy consumed for melting the feedstock and the attained deposition rate. The twin-wire arc-spraying (TWAS) process is thus the most economical coating process among the thermal-spraying techniques with respect to the above mentioned reasons. In addition, by utilizing cored wires, the TWAS process exhibits the highest variety in feedstock. Coatings produced by means of TWAS show

some disadvantages such as high porosity, high oxidation, limited reproducibility, and low adhesion strength. The attainable coating quality is controlled by the temperature, size, and velocity of the in-flight particles at impact (Ref 1-7).

The particles in the TWAS-spraying plume are initiated and formed through the atomization of a molten feedstock. The atomization occurs by the impingement of a fast and continuously flowing atomization gas jet (mostly compressed air) upon the melting wire tips of consumable electrodes. The wires as shown in Fig. 1 (one connected as anode (+) and the other one as cathode (−)) are fed together to ignite an arc at the shortest distance between the electrically conductive part in the wire tips. Besides the mass flow and velocity of the atomization gas, the type of gas used plays a dominant role on metal atomization. The higher viscous drag forces of heavy gases, such as argon, compared to that of lighter gases, such as nitrogen, could improve electrode atomization (Ref 1).

The arc fluctuations, caused by the periodic removal of molten droplets from the electrode tips, have also a strong effect on the droplet formation, and therefore, on the coating properties such as porosity, microstructure, and oxide content (Ref 2-7). Stanisic et al. (Ref 8) studied the atomization behavior in a TWAS/HVOF hybrid thermal-spraying process. The arc fluctuations in the hybrid process turned out to be smaller compared to that of the TWAS. Owing to the heated gap between the wire tips, the arc ignites even at a longer distance.

In general, droplet breakup in liquids occurs with the initiation of a disturbance on the liquid surface, which is enhanced by aerodynamic forces, leading to the formation of ligaments (origin of large droplets) and membranes (formation of smaller droplets). There is a direct shearing action which is a function of the velocity difference between the air and the liquid. One of the most important

W. Tillmann and **M. Abdulgader**, Institute of Materials Engineering, Technische Universität Dortmund, Dortmund, Germany. Contact e-mail: Mohamed.abdulgader@udo.edu.
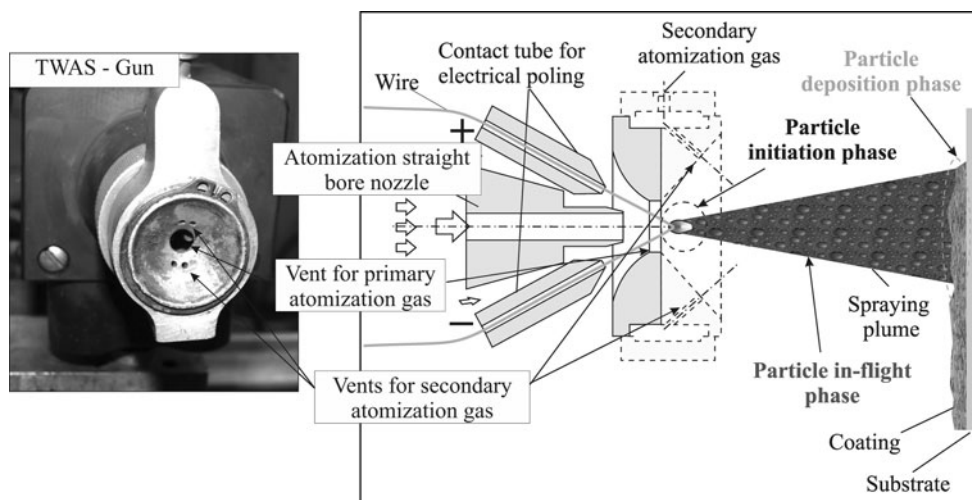
Fig. 1 Twin-wire arc-spraying process

parameters for describing droplet breakups from liquids or liquefied metals is the Weber number (Ref 9-11). In this paper, the term ''liquefied metal'' refers to metal heated above its melting point. The high surface tension of liquefied metals, used to fabricate fine metal powders, makes them difficult to atomize. Usually, supersonic gas velocities are employed in the metal powder production. Mates and Settles (Ref 10, 11) reported that an increase in the atomization pressure increases both the magnitude of the aerodynamic force available for disintegrating liquefied metal droplets (with or without building of metal sheets) and the distance over which this force is maintained at a high level.

The atomization process in the TWAS process is similar to the liquefied metal atomization in metal-powder production processes. Nevertheless, it remains distinctly different since the liquefied metal is not delivered in a continuous stream in the form of jets or sheets co-flowing with the atomizing media (Ref 9). The particle formation process is based essentially on the disintegration of the liquefied metal extrusions directly behind the electrodes as clearly shown in Fig. 2.

The ratio of gas/metal flow is one of the main distinctions between metal atomization in the TWAS process and molten metal atomization. The ratio in the TWAS process is controlled by the amount of molten wires per arc ignition and the sequence of the arc re-ignition. In addition to the fluctuating induced heat, the specific properties of the metal melt and the presence of solid cylindrical obstacles (spray wires) in the flow field make the atomization in the TWAS process more complicated than that of molten metals. Another inherent feature of the TWAS process is the different arc attachment to the electrodes (Ref 2-7, 12-18). In the case of the anode, the diffuse arc attachment heats a large part of the wire tip surface, creating a small layer of molten metal on the wire tip. The atomizing gas stream pushes the molten metal layer, creating a wave that carries the metal to the edge of the wire tip to create the anode sheet. The diffuse anode
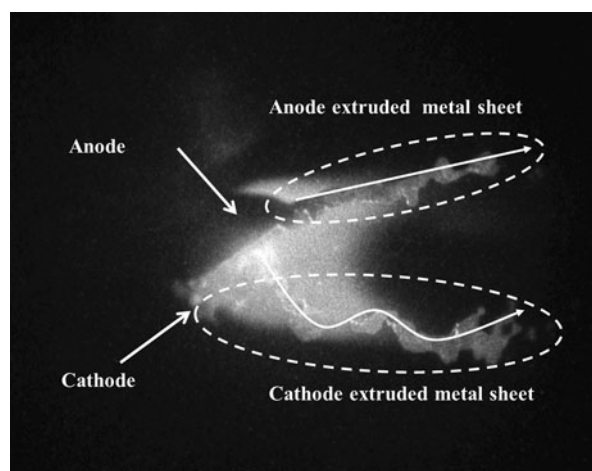

Fig. 2 Metal break up and melting behavior in the TWAS process (image was taken from the anode side)

attachment tends to move downstream spreading itself to the continually stretching anode sheet (Ref 10). Even though the consumption of anode and cathode is uniform, yet the burning of both electrodes is different. Steffens (Ref 13) found that the anode is burning in a sharp form while the cathode is burning obtusely.

Hussary and Heberlein (Ref 14) found that the structures of molten metal extrusions, formed at the edges of the electrodes, are a combination of sheets, membranes, and small extrusions. They categorized the breakup of molten metal structures into three types: (1) Rayleigh axisymmetric breakup; (2) Rayleigh non-axisymmetric breakup; and (3) membrane type breakup. The complex flow structure generated in the jet shear layer leads to bends in the molten metal sheet and a flapping movement as the sheet breaks up. Such a mechanism is termed as the Rayleigh non-axisymmetric breakup type. Disturbances on the molten metal/gas interface are amplified leading to the formation of the Kelvin-Helmholtz-type instability.

The amplified Kelvin-Helmholtz instability breaks the molten metal sheet into droplets with trajectories parallel to the jet axis. Such a breakup mechanism is referred to as the Rayleigh axisymmetric breakup type. The membrane type breakup can be observed when the extracted metal sheet at the edge of the electrodes is stretched to a point where a hole starts to form at its center. Owing to its high viscosity and high surface tension, the molten metal ultimately starts to collect at the rims of the membrane and around the newly formed holes forming a molten metal ring. The initiated molten metal ring directly disintegrates in the flow direction with either the Rayleigh axisymmetric or Rayleigh non-axisymmetric breakup (Ref 14).

The control over the in-flight particle characteristics is a very important topic in thermal-spraying processes (Ref 4). This enables us to meet the industrial demands regarding the prediction and the reproducibility of the desired coating quality. Furthermore, particle characteristics are dependent on the proceeding melting and atomization behavior of the type of feedstock used. Therefore, the aim of this research is to clarify the processes involved in the melting behavior and atomization in the TWAS process using solid and cored wires. The main focus of this study is to investigate the effect of the filling powder in cored wires on the melting behavior, droplet formation, and process instability. Thus, to the best of our knowledge, the melting behavior of cored wires is not yet thoroughly documented. The findings could serve in the accurate modeling and simulation of the TWAS process as well as in the modification of the atomization nozzles.

2. Experimental Setup

A TWAS system (Smart Arc 350 PPG, Sulzer Metco, Switzerland) was used to investigate the melting behavior of the feedstock during the TWAS process. The investigation was carried out on two types of wires with a diameter of 1.6 mm. The wires used were cored wires (DURMAT AS850, Durum, Germany) with the composition (in wt.%) of Cr 4%, Mn <1%, Si 1.4%, C 2%, WSC (fused tungsten carbide WC-W_2C) 50%, Fe Bal., and solid wire (Sprasteel 11, Sulzer Metco, U.S.A.) with the following composition (in wt.%) of Fe Bal., C 0.07%, Si 0.96%, Mn 1.63%. To study the effect of the filling powder on the melting behavior of the cored wire AS850 with an undefined powder size distribution, standard spray parameters supplied by Durum were used. Its melting behavior was set in comparison with that of the solid wire to clear the effect of filling powder on the melting behavior and particle formation. Compressed air was used as an atomizing gas. The melting behavior and particle formation process were recorded by a 12-bit high-speed camera (HSC) (type HSFC PRO, PCO, Germany). This camera is made up of four recording modules and can record 333 mfps (million frames per second). The exposure time was set to 100 ns and the delay time to 500 ns. In studying the melting behavior in the TWAS process, images were illustrated from the cathode side as well as from the anode side. In the case of cored wire, images were also taken from the upper side of the gun to explore the intersection area between the two electrodes. All experiments were performed without the illumination of the arc zone. This gave us the possibility to investigate the formation of smaller particles as well as to describe the phenomena occurring in arc ignition and re-ignition. Figure 3 shows the gun configuration and the locations of the HSC. Each recorded film contains about 164 images. The representative images were compared in order to investigate the influence of the spraying parameters and the presence of filling powder on the melting behavior and particle formation. The selected images are the ones with the higher repetition.

The following four independent adjustable process parameters were individually changed: primary atomization gas pressure PG (from 0.2 to 0.6 MPa), secondary atomization gas pressure SG (from 0 to 0.6 MPa), arc voltage U (from 28 to 32 V), and arc current I (from 180 to 260 A). Immediately after the high-speed images were taken for each parameter setup, the wire tips were cut for investigation. A light microscope (Axiophot, Co. ZEISS) was used to illustrate the effect of the adjustable process parameters on the wire tips. A field emission scanning electron microscope (JSM 7001F, Co. Jeol) equipped with an energy dispersive x-ray spectrometer (EDX) was used to study both, the morphological and topographical surfaces of wires used, and also the qualitative and quantitative elemental analysis in the wire melting zone. In addition, SEM observations of the contact point of the used wires were made to illustrate the effect of filling powder on metal extrusion by cored wires.

3. Results

The melting behavior of the feedstock in TWAS is a controlling factor in process performance. The type of the wires used affects directly the process stability. Two kinds of forces impact simultaneously on the wire tips in the TWAS process. The first one is the continuously operating aerodynamic force applied by the primary atomization gas pressure. The other one is the alternating heating caused by a fluctuating electrical arc because of the material removal from the wire tips by means of the atomization gas and the continuous feeding of the wire into the arc zone. The extinction and re-ignition of the arc occurred periodically in milliseconds (Ref 14).

3.1 Melting Behavior of Solid Wires

In the extracted HSC images, the side (electrode) from which the images were taken appears dark, while the counter-electrode is illuminated brightly. The captured images show a typical representation of metal breakups and particle formation from solid wires. For a better description of the metal breakups from the electrodes, a series of representative images of the individual HSC-records at the anode and the cathode were compared as
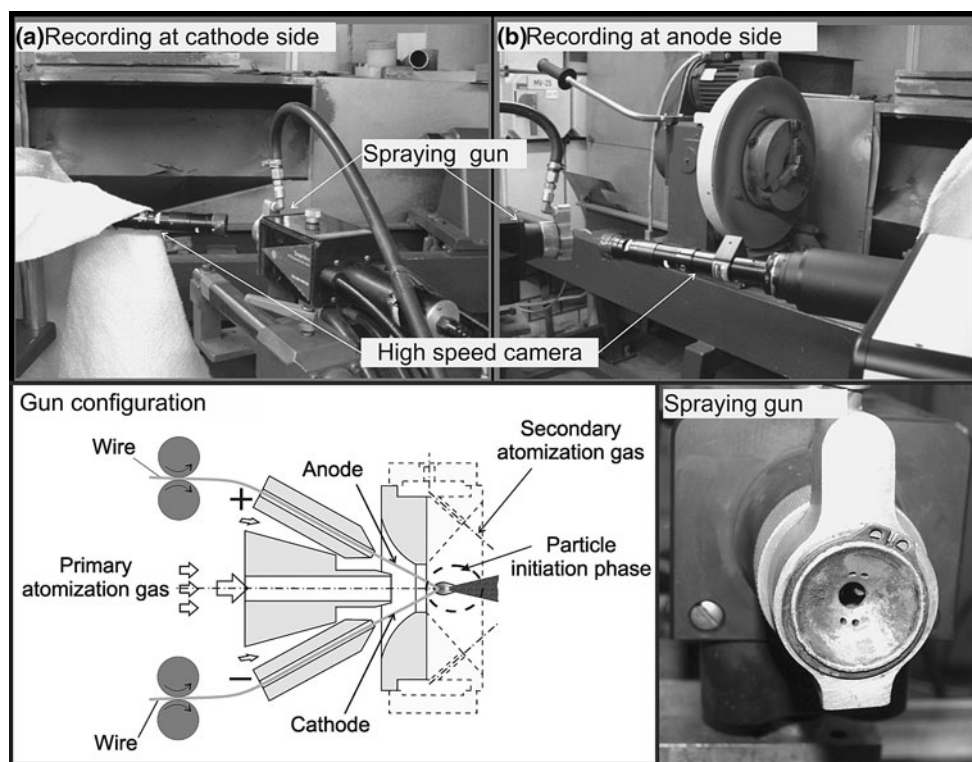
Fig. 3 Recording positions of the high-speed camera (a) at the cathode side (b) at the anode side
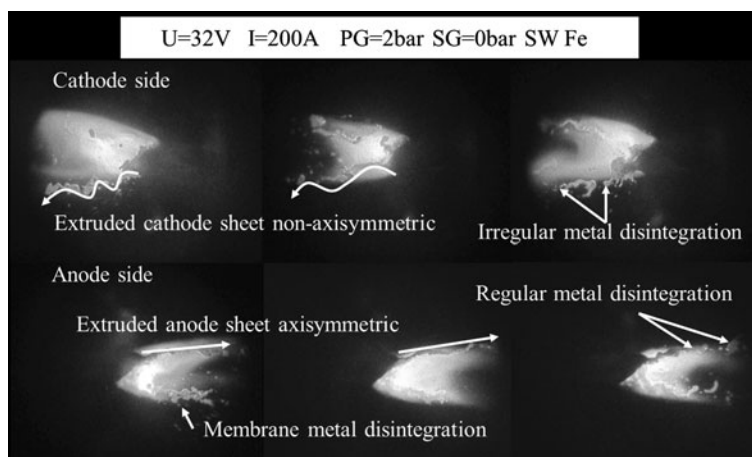

Fig. 4 Melting behavior and metal disintegration at the cathode and anode using solid wires

shown in Fig. 4. It is obvious that a continuous and relatively linear metal sheet is formed at the anode. The metal sheet extrusions at the cathode are nonlinear and in some places, strongly squeezed, which leads to disintegrations of a metal melt with irregularly shaped membranes from the cathode side. It is clear that some of the droplet disintegration is caused by the deformation of the extruded metal sheets.

Owing to the different heating of both electrodes, the shape of the extruded metal sheets from the anode and cathode varies. At the cathode, a constricted arc attachment causes much more localized heating and melting. The temperature of the molten material from the cathode is higher than that from the anode. Accordingly, and due to the Eötvös rule (surface tension decreases with increased temperature), the droplets initiated from the cathode are smaller than the ones initiated from the anode. The higher temperature of the extruded metal sheet at the cathode could also be the reason for the dominance of non-axisymmetric liquid metal breakup at the cathode. The

symmetry of the wire intersection in the gas flow lets us arrive at the conclusion that the Karman vortex streets behind the electrodes affect the extruded metal sheets with similar impact. Therefore, the variations in the shapes of the extruded metal sheets of the individual electrodes are only due to the variation in their temperature.

The arc re-ignition occurred between the electrode tips as well as between the extruded metal sheets of the electrodes. The recorded high-speed films reveal a moving arc along the metal sheets. Such arc movement causes extensive heating of a larger area downstream of the intersection between the electrodes. The re-ignition of a moving arc is very likely to take place between the ends of the extruded metal sheets. The re-ignition causes a sudden heating of the extruded metal sheets and leads to metal disintegration in a regular form (droplets) or an irregular form (membrane) and causes the breakup of the sheets. The images describing these phenomena were taken from two successively recorded sequences of the four camera modules. Considering Fig. 5, the upper images show arc ignition between the electrode tips. From the lower images shown in Fig. 5, it is observed that the arc was re-ignited between the extruded metal sheets.

Almost all images revealed a unique characteristic of the extruded metal sheets at the anode and the cathode. While the extruded metal sheet at the cathode points downward, the anode sheet points straight forward with a tendency of upwards direction. Besides the variation in the metal sheet temperatures between the anode and cathode, the acting magnetic forces could be a possible explanation for this behavior.

3.1.1 Effect of the Primary Atomization Gas Pressure. The level of primary atomization gas pressure is one of the major factors affecting the length of the extruded metal sheets. Besides the heating of feedstock material due to the arc ignition and re-ignition, any changes in the acting aerodynamic forces lead to a variation in the length of the extruded metal sheets (Fig. 6). The higher PG causes a decrease in the length of the extruded metal sheets and increases the vertical distance between the sheets. The reason for that could be the large vortexes behind the electrodes at a higher PG. The larger vortexes lead to an excessive deformation and bending of the sheets resulting in a metal disintegration close to the parent wires. Owing to the variation in the temperature of the metal sheet at the anode and cathode, a metal disintegration occurring earlier from the cathode metal sheet was observed. The PG also affects the shape of the metal disintegrations. At a lower PG, the metal disintegrations have almost an irregular shape (large membranes). In the case of a higher PG, the shapes of the metal disintegrations become more regular and vary between small membranes and droplets.

3.1.2 Effect of the Current. The wire feed rate is adjusted to the current level. Very high current level leads to an increase in wire feed rate. The induced heat is not high enough to liquidize all the material fed in the arc zone. Therefore, the amount of doughy material (softening of the metal due to a higher temperature) at the wire tips is increased and thus the length of the extruded metal sheets. Figure 7 shows the variations in the length of the extruded metal sheets according to the variation in current. Doughy material is a material state caused by the heat propagation in metals. The temperature of doughy material is directly below the melting point of these materials. In this paper, the term is used to describe the wire material at an elevated temperature.

The length of the extruded metal sheet at higher current is about three times the diameter of the wire used. The metal disintegrations reveal an elongated membrane form at the end of the metal sheets. The arc-moving zone becomes larger with the greater length of the extended metal sheets. Therefore, arc-exposed area is consequently increased. The disintegrated metal is to some extent regular shaped and varies from medium to small membranes. In the case of a lower current, the disintegration occurs closer to the parent wires.
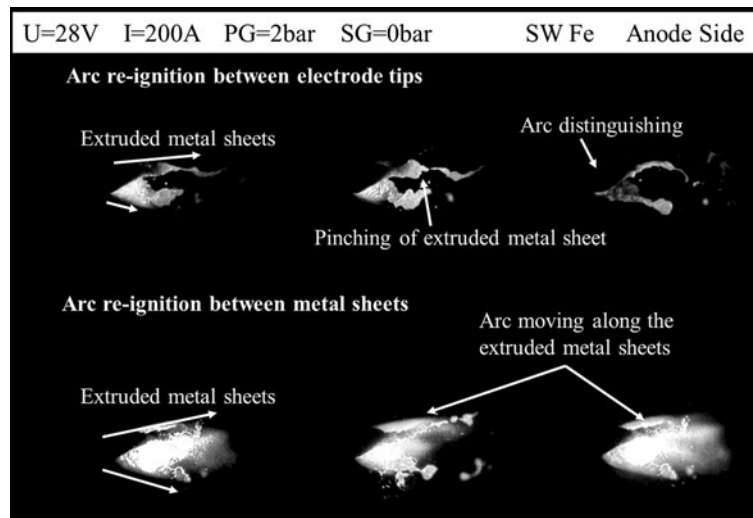

Fig. 5 Re-ignition and moving of the arc between extruded metal sheets
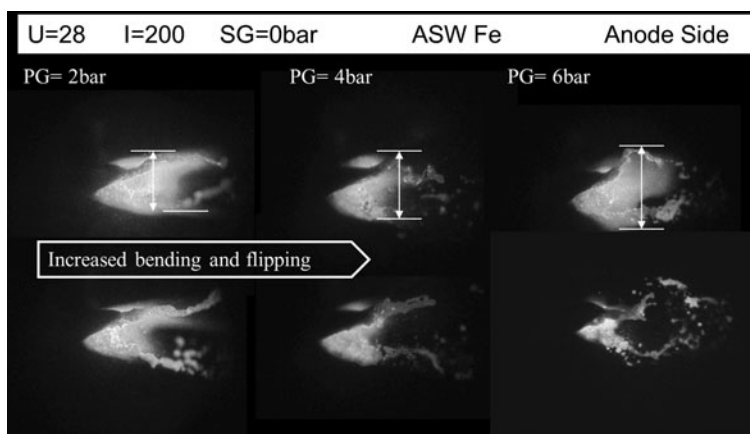
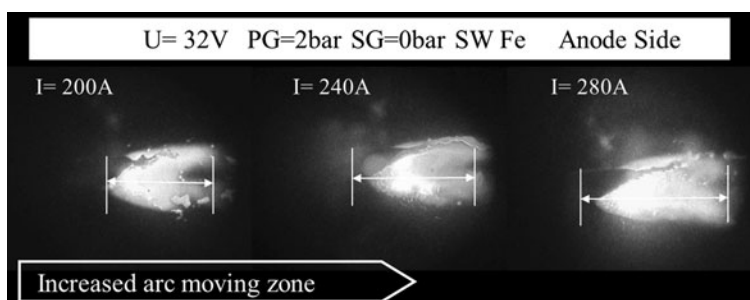**Fig. 6** Effect of the primary atomization gas pressure on metal sheet formation and metal disintegrations

Fig. 7 Effect of the current (I) on the arc moving zone

3.1.3 Effect of the Voltage. Induced heat and aerodynamic forces are the determining factors controlling the melting behavior and particle formation. The interplay between these forces governs the shape and size of metal disintegrations. With an increased voltage, the induced heat was also increased. The increase in voltage even at lower PG led to a decrease in the length of the extruded metal sheets. The reason for that could be the ihigher temperature of the doughy part at higher voltage level. The higher temperature of the doughy part improves its deformability, which leads to a metal disintegration closer to that the parent wires. At a low voltage of $U = 28$ V, a greater sheet length was recorded. The metal disintegration occurred at a distance 1.5 times the diameter of used wire. At higher voltages, the metal disintegration was closer to the parent wires. The brightness of the arc at $U = 32$ V indicates the heat intensity of the arc at this setting.

3.2 Melting Behavior of Cored Wires

The cored wires are a combination of two kinds of feedstock used in thermal spraying (wires and powders). The sheath of the cored wires is made of electrically conductive, deformable metals. The core is filled with powders of non-conductive or non-deformable materials such as metal carbides or oxides. The content of the cored wires can be individually tailored to fulfill the industrial applications. Owing to the presence of filling powders in the cored wires, their melting behaviors and metal disintegrations are different from those of the solid wires as shown in Fig. 8.

The images recorded from both sides reveal no specific shape of the extruded metal sheets in the axial direction. The metal disintegration occurs without the building of any metal extrusion especially at the anode side. The reason for the missing formation of the metal sheets is the cross-sectional area of the electrically conductive sheath. The surface area of the conductive part of a 1.6-mm diameter solid wire is about 2 mm^2 compared to 0.38 mm^2 in the case of a 1.6-mm diameter cored wire. The calculation of the surface area of the conductive part of the cored wire was made for a sheath thickness of 0.08 mm. Therefore, the amount of the doughy part of the molten metal in the case of cored wires is much smaller than that of solid wires.

In the case of cored wires, the ignited arc heats the facing surfaces of the wires and melts them. The liquefied metal is directly atomized and blown away by the gas stream. At the same time the doughy parts of the wires are extruded and form the metal sheets. A part of the filling powder is melted and removed along with the extruded doughy metal as shown in Fig. 9.

The remaining parts are set free and therefore exposed to the atomizing gas flow. The remaining filling powder is
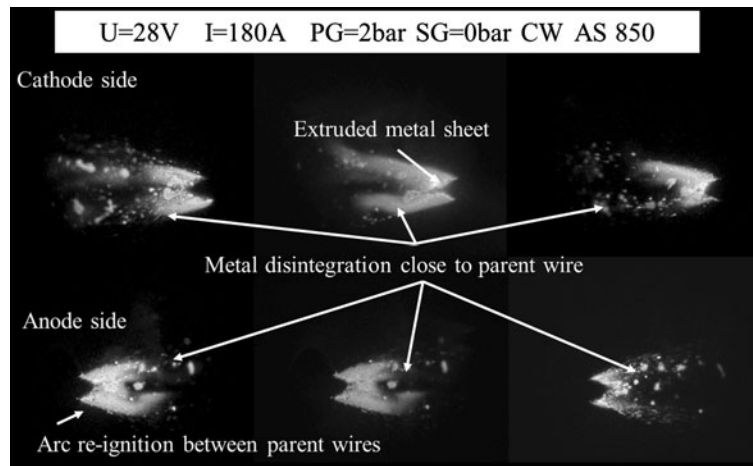
Fig. 8 Melting behavior and metal disintegration at the cathode and anode using cored wires
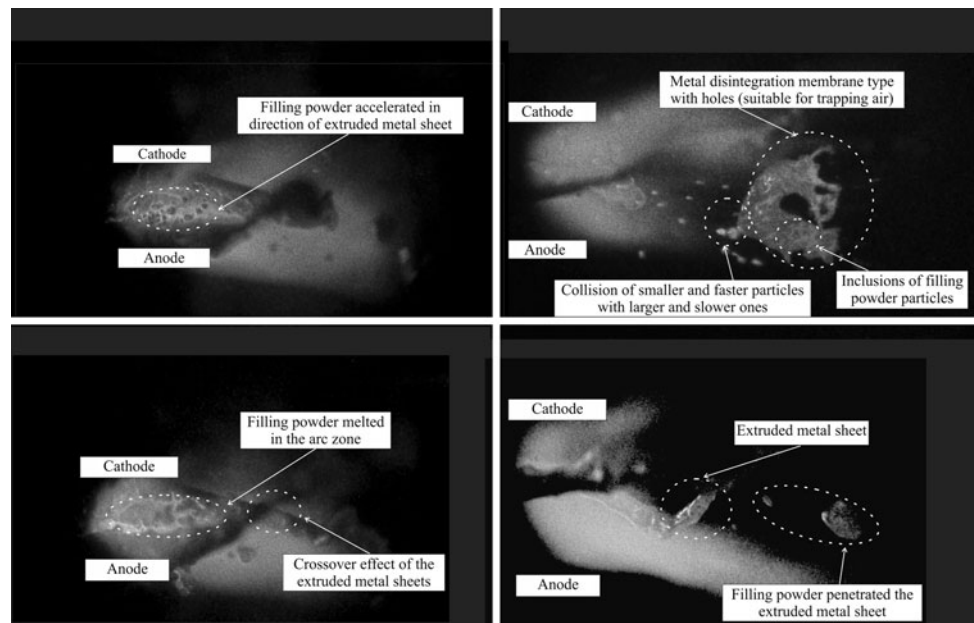

Fig. 9 Images from upper side showing the effect of the filling powder on melting behavior and metal disintegrations

eroded by means of the continuously flowing atomizing gas. The powder particles are accelerated in the direction of gas flow. In their flight path, they penetrate against the extruded metal sheets and cause metal disintegrations near the parent wires as shown in Fig. 9. Consequently, the penetration causes a breakup of the extruded metal sheets.

The solidified metal sheets, after the arc extinguishing, are shown in Fig. 10. The images clearly show the effect of the filling powder on the metal disintegration by cored wires. The presence of powder particles in the leftover molten part revealed an impingement of the powder particles with the extruded metal sheets. The images strengthen the finding made by Steffens in Ref 13 that the anode is burning in sharp form (with a sharp angle) while

the cathode is burning in an obtuse form (flat edge). The sharpness is increasing with higher atomization gas pressure. The leftover melt is higher at the anode side. The reason for this could be the higher temperature at the cathode side, which leads to a lower surface tension (Eötvös rule), thereby making the atomization of liquefied material easier. The higher leftover melt in the case of PG = 0.6 MPa is due to the exothermic reaction and the higher aerodynamic forces applied pushing the melt through the filling powder.

The rapid cooling of the melting bath leads to short diffusion times between metal matrix and the filling powder. The molten part of the filling powder dissolves in the metal melt forming intermetallic compounds. The solidification mechanisms are dependent on the concen-
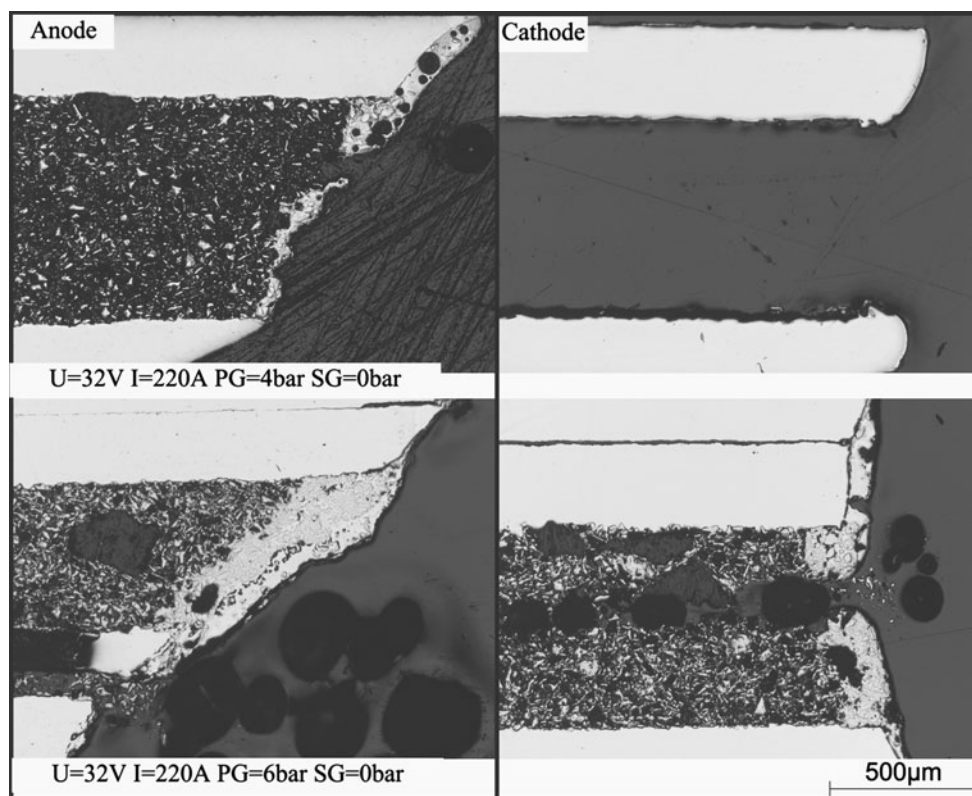
Fig. 10 Cross sections of the used cored wires

tration and the number of the components, which are pronounced strong carbide-forming elements in the melt. The time during which the compound remains in its molten state is very short. For in-flight particles with a velocity of 150 m/s and a substrate stand-off distance of 130 mm, the time is about ~0.85 ms. Owing to the short existence time of the compounds in a molten state, the diffusion is restricted. A part of the dissolved tungsten could alloy substitutionally and form solid solution with iron. As the tungsten-iron alloy starts to solidify, the tungsten tends to form carbides, Fig. 11.

The arc heats the used wires, because of the thermal conductivity of metals, in three different zones. Figure 12 clearly shows the three different arc heated zones of the wires.

The first zone is the intersection surface of the wires, which is directly exposed to the arc ignition or re-ignition. Owing to the induced heat, this area consists of fully liquefied metal. The depth of this zone depends on the magnitude of the induced heat and the melting point of the materials involved. The presence of solidified droplets at the wire surface is evidence of liquefied metal (Fig. 12a, b). The holes in Fig. 12(d) are a sign of escaped bubbles caused by boiling metal. The thermal conductivity of the metals causes a heat transfer to the boundary layers. These layers reach a temperature which is high enough to generate a doughy metal area. The solidified metal sheets are evidence for the presence of easily deformable doughy metal (Fig. 12e). The temperature of the wires at deeper

layers (at the doughy area bordering layers) is decreased. Nevertheless, the temperature is still high enough to enable a permanent deformation at the wire tips. This is due to the acting aerodynamic forces (Fig. 12f).

4. Summary and Discussion

Detailed knowledge of the melting behavior and particle formation is very important for the modeling and the simulation of a TWAS process. In addition, it helps to accomplish the desired modification of the spraying nozzles. The investigations show that the kind of wires used and adjustable process parameters are the determining factors controlling the metal disintegration. The thermal exchange phenomena in the arc zone are very complicated. On one hand, we have a fluctuating arc. As the arc ignites, it heats the feedstock and causes the metal to melt or even to boil. On the other hand, we have a fast and permanent flow of pressurized air; which simultaneously causes a continuous cooling of the molten metal. The gas flow removes the heated part of the wire tips, which leads to the extinguishing of the arc. As the gap between the approaching electrodes becomes shorter, a re-ignition of the arc occurs between either the wire tips or the extruded metal sheets, so long as the extruded metal sheets are connected to parent wires.

The arc re-ignition occurs at the shortest distance between the two electrodes. Owing to the intersection
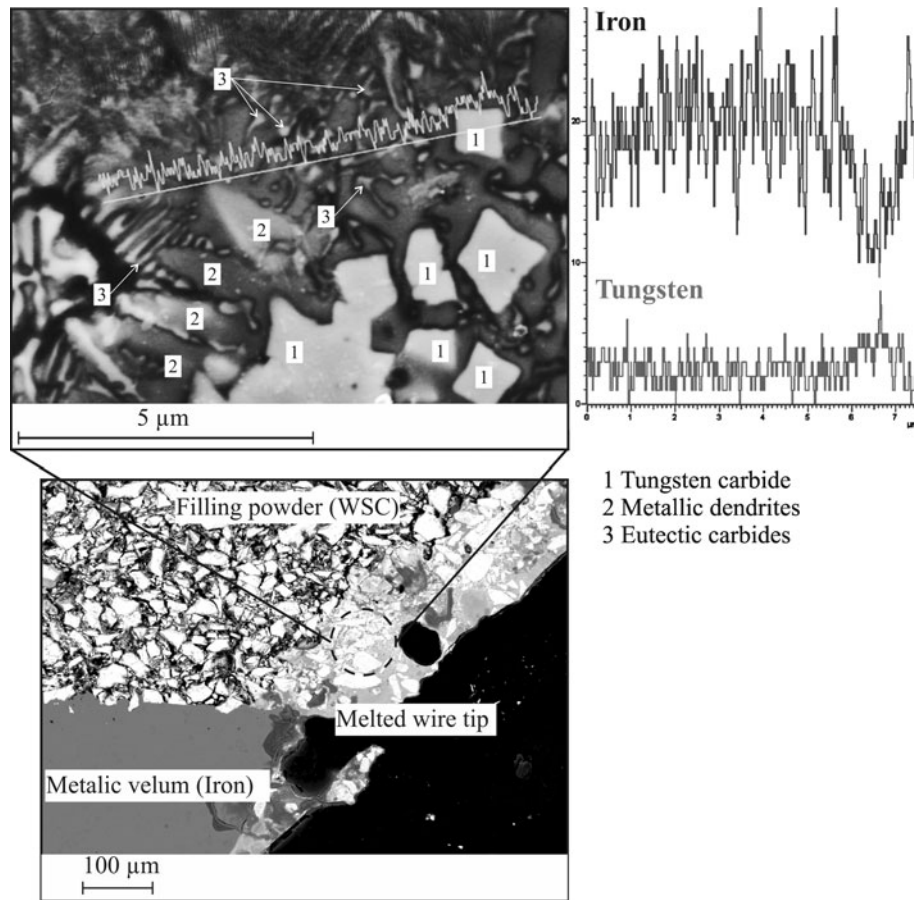
Fig. 11 Element mapping of a SEM-cross sections of the cored wires

angle between the electrodes with its slope toward the gas flow direction, the extruded metal sheets play a crucial role for the arc re-ignition. The re-ignition leads to an excessive heating of the metal sheets. The increase of the temperature of the molten metal, according to the Eötvös rule, causes a decrease in its surface tension. This enhances the formation of regular metal disintegrations in the form of smaller droplets. We believe that the actual melting (phase change) and thus the existence of a higher amount of liquefied material occurs only during the time of the arc ignition or re-ignition. Owing to the thermal conductivity of the wires, the arc heats the wires in three different zones. The first zone is the contact surface of the electrodes (or at extruded metal sheets). The arc ignition or re-ignition causes the material in this zone to melt or even to boil. The second zone is the area directly below the liquefied material. This area becomes doughy and thus can easily deform. The third affected area is the area directly below the doughy area. The metal temperature in this area is high enough to permanently deform the electrodes at the gas flow intersection. The gas flow at the liquefied material area causes metal disintegrations in the form of smaller droplets. The size of these droplets is a function of the temperature of the liquefied material and the aerodynamic forces (Eötvös rule and Reynolds number). The doughy area is the origin of the extruded metal

sheets. The length of the extruded metal sheets is also a function of the temperature of the doughy area and the aerodynamic forces caused by the gas flow. It can reach approximately three times the diameter of the used wire. Because the gas flow is permanent, it is believed that the existence of the extruded metal sheets is also permanent. It is the length of these sheets that is changed, with a depends on the arc ignition. Their breakup is dependent on the temperature of the doughy area and the aerodynamic forces. The arc could re-ignite between the extruded metal sheets and move along them. The shapes of the extruded metal sheets (axisymmetric or non-axisymmetric) are mainly caused by the effects of Karman vortex streets behind the electrodes more than by those of Kelvin-Helmholtz instability, which can be due to two factors: . On the one hand, the extruded metal sheets do not act as liquefied (molten) material but they behave like doughy heated metal. On the other hand, the gas ratio is higher compared with the liquefied metal as the gas flow is permanent, yet the heating source (the arc) required to melt the wires is fluctuating. In addition, the cross-sectional area of the wires is very small. Therefore, the amount of gas flow is much higher than the available liquefied metal.

The variations in the shape of extruded metal (axisymmetric, non-axisymmetric, or membrane) are due to
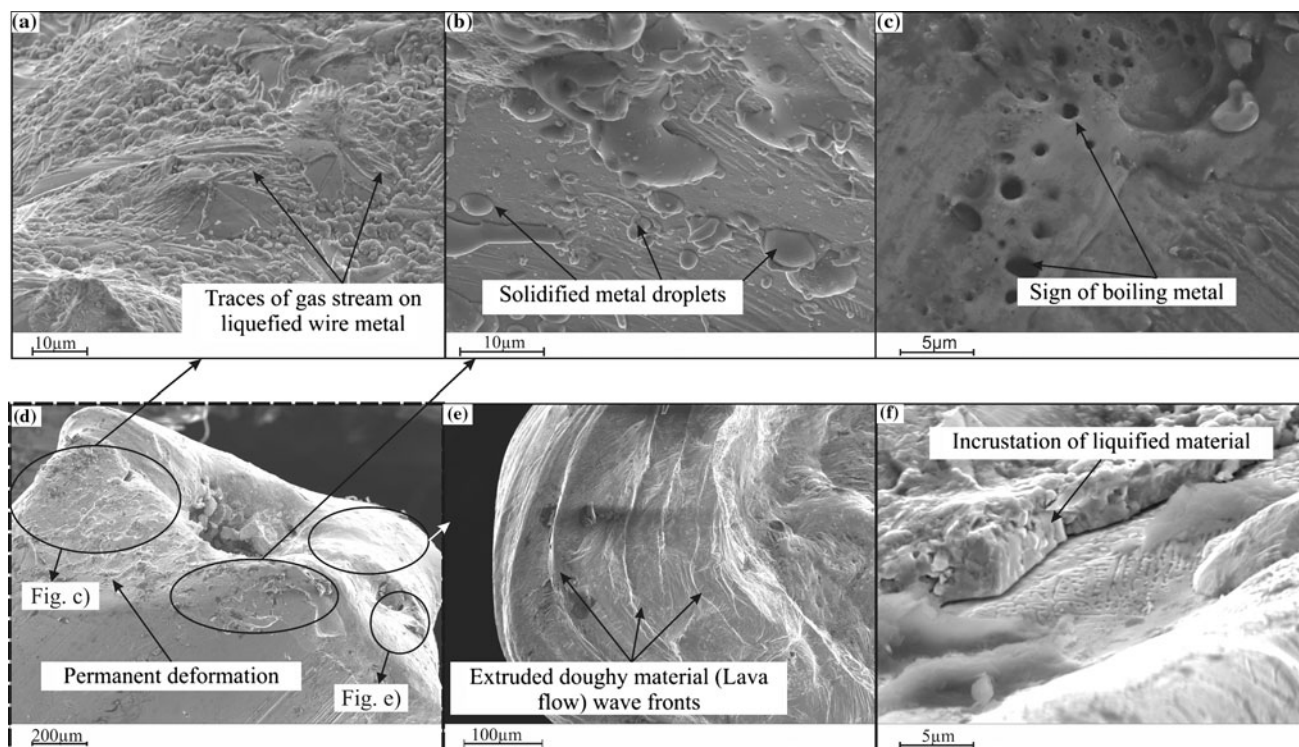
Fig. 12 SEM images showing the different zones of the heated electrodes in the TWAS process. (a) Traces of solidified liquid metal flow, (b) solidified metal droplets, (c) solidified crust of metal liquid, (d) holes indicating bubbling effect of boiling metal, (e) Doughy metal (erupted magma) building the extruded metal sheet, and (f) deformed wire tip
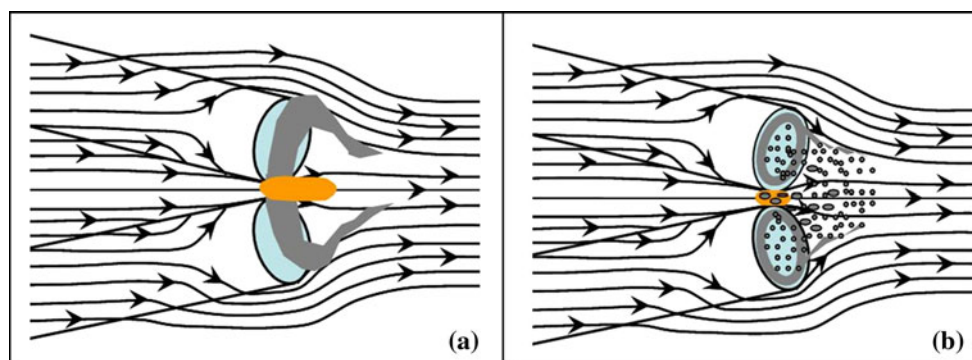

Fig. 13 Melting behavior and metal disintegration of (a) solid wire, and (b) cored wires

the well-known asymmetric melting behaviors of anode and cathode (Ref 2-7, 12-18). At the cathode, a constricted arc attachment causes greater localized heating and melting of the feedstock. In the case of the anode, the diffused arc attachment heats a large part of the wire surface, creating a small layer of molten metal of the feedstock. This leads to a variation in the heating of the anode and cathode. The molten material as well as the doughy part at the cathode would have a higher temperature than that at the anode. This can be verified (more obviously in the case of solid wire) by the length of the metal sheet at the anode, which is greater than that of

the cathode. Therefore, the extruded metal sheets at the cathode are ruptured more easily.

In the case of cored wires, the ignited arc heats the facing surfaces of the wires and melts them up, while liquefied metal is directly atomized and blown away by the gas stream. At the same time, the doughy parts of the wires are extruded and form the metal sheets. A part of the filling powder is removed along with the extruded doughy metal. The remaining parts are set free, and therefore, exposed to the atomizing gas flow as shown in Fig. 13. The remaining filling powder particles are eroded by means of the continuous flowing atomizing gas and are

accelerated in the direction of gas flow. On their way, the powder particles penetrate the extruded metal sheets and cause the metal disintegrations near the parent wires. The penetration consequently causes a breakup of the metal sheet.

5. Conclusions

The melting behavior of cored wires was compared to that of the solid wires to investigate the effect of the filling powder on the melting behavior and the particle formation. The filling powder in cored wires plays a decisive role in the metal disintegration (particle formation) in a TWAS process. They are responsible for the metal disintegration directly behind the parent wires. The extruded metal sheets of both anode and cathode are shorter than the ones observed for solid wires. The metal disintegration, in the case of cored wires, shows almost regularly shaped membranes and droplets. Some of the irregularly shaped disintegrations were observed directly behind the parent wires. At higher voltage settings, the number of the irregular disintegrations is higher. The size of these droplets is a function of the specific properties of the metal melt (i.e., surface tension, dynamic viscosity, heat conductivity) and the acting dynamic forces, and, in the case of cored wires, the particle size distribution of the filling powder.

The recorded images indicate a wider arc caused by the cored wires. The arc in the case of cored wires shows a curvature-shaped outer edge causing a higher jet divergence. The images of the droplets formed in the case of cored wires exhibited mostly the absence of the extruded metal sheets at the cathode and anode side. The extruded metal sheets, to some extent, support the re-ignition of the arc and enhance the process stability in TWAS. Therefore, the cored wires are more sensitive to changes in the process parameters. An optimal fit between the velum materials, velum thickness, and the grain size of the filling powder should be worked out for more stable TWAS processes using cored wires.

Acknowledgments

References

1. D. Sacriste, N. Goubot, J. Dhers, M. Ducos, and A. Vardelle, An Evaluation of the Electric Arc Spray and (HPPS) Processes for the Manufacturing of High Power Plasma Spraying MCrAlY Coatings, *J. Therm. Spray Technol.*, 2001, **352**, p 35-358
2. H.L. Liao, Y.L. Zhu, R. Bolot, C. Coddet, and S.N. Ma, Size Distribution of Particles from Individual Wires and the Effects of Nozzle Geometry in Twin Wire Arc Spraying, *Surf. Coat. Technol.*, 2005, **200**, p 2123-2130
3. A. Newbery, P. Grant, and T. Neiser, The Velocity and Temperature of Steel Droplets during Electric Arc Spraying, *Surf. Coat. Technol.*, 2005, **195**, p 91-101
4. A. Pourmousa, J. Mostaghimi, A. Abdini, and S. Chandra, Particle Size Distribution in a Wire-Arc Spraying System, *J. Therm. Spray Technol*, 2005, **14**(4), p 502-510
5. M.P. Planche, H. Liao, and C. Coddet, Relationships Between In-Flight Particle Characteristics and Coating Microstructure with a Twin Wire Arc Spray Process and Different Working Conditions, *Surf. Coat. Technol.*, 2004, **182**, p 215-226
6. T. Watanabe, T. Sato, and A. Nezu, Electrode Phenomena Investigation of Wire Arc Spraying for Preparation of Ti-Al Inter-Metallic Compounds, *Thin Solid Films*, 2002, **407**, p 98-103
7. A.P. Newbery, T. Rayment, and P.S. Grant, A Particle Image Velocimetry Investigation of In-Flight and Deposition Behavior of Steel Droplets during Electric Arc Spray Forming, *Mater. Sci. Eng.*, 2004, **A383**, p 137-145
8. J. Stanisic, D. Kosikowski, and P.S. Mohanty, High-Speed Visualization and Plume Characterization of the Hybrid Spray Process, *J. Therm. Spray Technol.*, 2006, **750**(15), p 750-758
9. A. Mansour and N. Chigier, Disintegration of Liquid Sheets, *Phys. Fluids*, 1990, **A2**, p 706-719
10. S.P. Mates and G.S. Settles, A Study of Liquid Metal Atomization Using Close-Coupled Nozzles, Part 1: Gas Dynamic Behavior, *At. Sprays*, 2005, **15**(1), p 19-40
11. S.P. Mates and G.S. Settles, A Study of Liquid Metal Atomization Using Close-Coupled Nozzles, Part 2: Atomization Behavior, *At. Sprays*, 2005, **15**(1), p 41-60
12. N.A. Hussary and J.V.R. Heberlein, Effect of System Parameters on Metal Breakup and Particle Formation in the Wire Arc Spray Process, *J. Therm. Spray Technol.*, 2007, **140**(16), p 140-152
13. H. Steffens, "Haftung und Schichtaufbau beim Lichtbogen- und Flammspritzen, (Adhesion and Layer Structure for Arc and Flame Spraying)," Ph.D. thesis, Hannover Technical University, 1966 (in German)
14. N.A. Hussary and J.V.R. Heberlein, Atomization and Particle-Jet Interactions in the Wire-Arc Spraying Process, *J. Therm. Spray Technol.*, 2001, **10**, p 604-610
15. X. Wang, J. Heberlein, E. Pfender, and W. Gerberich, Effect of Nozzle Configuration, Gas Pressure, and Gas Type on Coating Properties in Wire Arc Spray, *J. Therm. Spray Technol.*, 1999, **8**(4), p 565-575
16. N. Hussary and J. Heberlein, *Metal Droplet Formation Mechanisms in the Wire Arc Spraying Process, 48*, Internationales wissenschaftliches Kolloquium, Illmenau, 2003, p 22-25
17. J. Wilden, J. Bergmann, S. Jahn, S. Knapp, F. van Rodijnen, and G. Fischer, Investigation about the Chrome Steel Wire Arc Spray Process and the Resulting Coating Properties, *J. Therm. Spray Technol.*, 2007, **16**(5-6), p 759-767
18. W. Tillmann, E. Vogli, and M. Abdulgader, Asymmetric Melting Behavior in Twin Wire Arc Spraying with Cored Wires, *J. Therm. Spray Technol.*, 2008, **17**(5-6), p 974-982